HTML ABSTRACT + LINKS

APPLIED PHYSICS LETTERS VOLUME 85, NUMBER 20 15 NOVEMBER 2004

Laser action in Eu-doped GaN thin-film cavity at room temperature

J. H. Park and A. J. Steckl[a)]
Nanoelectronics Laboratory, University of Cincinnati, Cincinnati, Ohio 45221-0030

(Received 30 July 2004; accepted 30 September 2004)

Rare-earth-based lasing action in GaN is demonstrated. Room-temperature stimulated emission (SE) was obtained at 620 nm from an optical cavity formed by growing *in situ* Eu-doped GaN thin films on sapphire substrates. The SE threshold for optical pumping of a ~1 at. % Eu-doped GaN sample was ~10 kW/cm^2. The SE threshold was accompanied by reductions in the emission linewidth and lifetime. A modal gain of ~43 cm^{-1} and a modal loss of ~20 cm^{-1} were obtained. © *2004 American Institute of Physics*. [DOI: 10.1063/1.1821630]

Trivalent rare-earth (RE^{3+}) ions exhibit inner-shell (intra-4f) transitions that produce sharp photoemission lines with wavelengths ranging from the ultraviolet to the near infrared. The RE^{3+} transition energies are independent of temperature in a given host and vary only slightly from host to host. The excitation efficiency and emission intensity do depend on the host material. *RE*-based emitters have found many applications:[1] phosphors for displays, solid-state lasers, and fiber-optic amplifiers. The *RE*-based solid-state lasers utilize an insulating host and are optically pumped. To achieve electrically pumped *RE* lasers requires a semiconductor host with certain properties: band-gap energy commensurate with the *RE* transition energy, good high electric-field properties, ability to introduce a significant *RE* density without luminescence quenching, ability to efficiently excite the RE^{3+} ions, etc. The major potential advantage of *RE*-based semiconductor lasers is an essentially fixed emission wavelength, which is defined by an *RE* atomic transition and does not vary with host material changes, optical cavity design, or operating temperature. While many semiconductor materials have been, and continue to be, investigated for this purpose, to date no conclusive reports of *RE* lasing in semiconductor hosts have been published.

One of the most promising semiconductor hosts for *RE* lasing is the wide band-gap semiconductor GaN. In addition to fulfilling the criteria listed above for *RE* hosts, GaN has been shown[2] to be produce outstanding "intrinsic" light-emitting diodes and lasers. Furthermore, the wide band gap and the ability to tailor the band-gap through III-N alloying enable matching this materials system to many RE^{3+} ions. Luminescence from GaN doped with Er, Eu, Pr, Tb, Tm, and other *RE*s has been reported.[3] In this Letter we report *RE*-based laser action in GaN.

Eu-doped GaN was grown on sapphire substrates (10 $\times$10 mm) in a solid source molecular-beam epitaxy system. An AlN buffer layer was grown for 5 min followed by the growth of GaN:Eu for 1 h, resulting in a 0.6-μm active layer doped with ~1–3 at. % Eu. A GaN cap layer was grown for 2 min. The substrate temperature was set at 800 °C during growth. Finally, the sample was annealed at 675 °C for 1 h. The detailed growth process of GaN *in situ* doped with Eu and other *RE*s has been previously reported.[4]

The basic configuration of threshold and linewidth measurements follows Amano *et al.*[5] A N_2 laser (λ=337.1 nm) with 600-ps pulse width and 10-Hz frequency was used as a pumping source. The pump beam is focused by a cylindrical lens to form a 10$\times$0.5-mm stripe on the sample surface. The sample edges were polished to reduce light scattering from the cleaved edge. The cavity length is held constant at 10 mm. Light emission from the top surface has spontaneous emission characteristics, whereas light emission from the film edge can contain both spontaneous and stimulated emission (SE). To insure that only edge emission is collected, another knife edge is placed perpendicular to the top surface blocking the surface emission.

The Eu^{3+} intra-4f transitions have several energy levels that can emit at visible wavelengths. The most commonly observed Eu^{3+} transitions are the $^5D_0$ to ^7F_J (J=0,1,2,3) levels generating red light, with the $^5D_0 \rightarrow {}^7F_2$ being dominant.

In this work, using GaN:Eu on sapphire, the $^5D_0 \rightarrow {}^7F_2$ transition is also dominant, with the emission peak at ~620 nm [Fig. 1(a)]. The Eu^{3+} ions in the GaN host are assumed to be primarily substitutional in Ga sites. In practice, various sites having distinct optical properties have been reported.[6–8] These local Eu^{3+} environments produce an inhomogeneous broadening of the Eu emission, which can be represented[9] by a Gaussian distribution. The dashed line in Fig. 1(a) is the Gaussian fitting of the dominant transition level. Edge emission from photopumped GaN:Eu shows a superlinear dependence on pumping peak power density [Fig. 1(b)], indicating the occurrence of SE. The SE onset occurs at ~10 kW/cm^2 peak power density. This value is very much lower than the SE threshold reported[10] for *RE*-doped noncrystalline materials (typically ~MW/cm^2). The linewidth of the Eu^{3+} emission below threshold is ~3.3 nm [Fig. 1(b)], dropping to ~2.0 nm above threshold. This linewidth reduction ratio of ~40% is higher than that reported[11] for Ce-doped δ-Al_2O_3 nanoparticles (~26%).

In general, for low threshold laser operation several characteristics are required:[12] large SE cross section (σ_{ex}), high absorption coefficient for optical pumping (GaN: ~10^5/cm at 337 nm), high excitation conversion efficiency, high radiative quantum efficiency (η), low thermal population of lower laser level (N_1), no (or low) excited-state absorption, and long photoluminescence (PL) lifetime.

The threshold power is inversely proportional[13] to the SE cross section (σ_{ex}) and the PL lifetime (τ_{PL}). σ_{ex} calculated by the integral β-τ method[14] is given by

[a)]Electronic mail: a.steckl@uc.edu

0003-6951/2004/85(20)/4588/3/$22.00 © 2004 American Institute of Physics
Downloaded 16 Nov 2004 to 129.137.207.245. Redistribution subject to AIP license or copyright, see http://apl.aip.org/apl/copyright.jsp

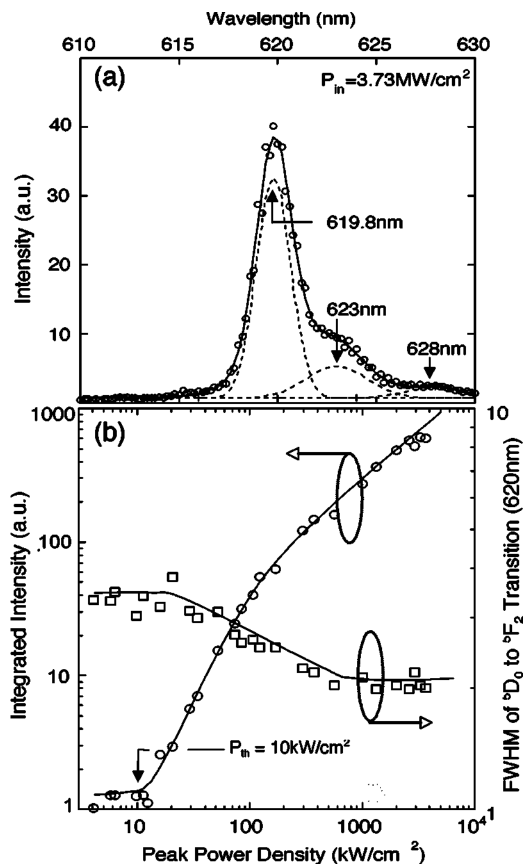

FIG. 1. (a) Spectrum of edge emission from GaN:Eu on Al_2O_3 substrate. (b) Integrated output intensity and spectral width as a function of input peak power density emission. SE threshold ~10 kW/cm^2.

$$\sigma_{ex} = \frac{\eta\lambda^5}{\tau_{\mathrm{PL}}[\int \lambda I(\lambda)d\lambda]8\pi n^2 c} I(\lambda), \quad (1)$$

where $\eta = \tau_{\mathrm{PL}}/\tau_R$ is the radiative quantum efficiency of the upper laser state, τ_R is the radiative lifetime, $I(\lambda)$ is the spectral emission intensity, c is the velocity of light in vacuum, and n is the refractive index of host material ($n \sim 2.3$ for GaN). The radiative transition of Eu^{3+} emission in GaN host is known[6] to be very strong, resulting in an RT value of $\eta \approx 0.9$. τ_{PL} of ~280 μs was experimentally obtained. The σ_{ex} at the peak wavelength is then calculated to be $\sim 6.8 \times 10^{-20}$ cm^2. This value is of the same order as that reported for *RE*-doped crystals[15] and ~10× higher than that found in *RE*-doped glasses.[16]

Since GaN:Eu exhibits strong Eu-related emission but no intrinsic (near-band-gap) emission under strong above-band-gap pumping, the excitation conversion process is very efficient. Another consideration is the thermal population of the lower laser level ($^7F_2$). This level is known[17] to be ~0.125 eV above the ground level. Therefore, the thermally induced population (N_1) of $^7F_2$ at RT is 100× smaller than that of the ground level. In this case the population inversion value is $\Delta N = N_2 - N_1 \approx N_2$ (the population of the higher laser level). This indicates that population inversion should be relatively easy to achieve.

Other factors to be considered are changes at the SE threshold in the lifetime at the peak wavelength and the polarization. Above threshold, a reduction of ~15% in the Eu^{3+} emission lifetime and a TE mode emission ~1.5× higher than TM mode emission were measured.

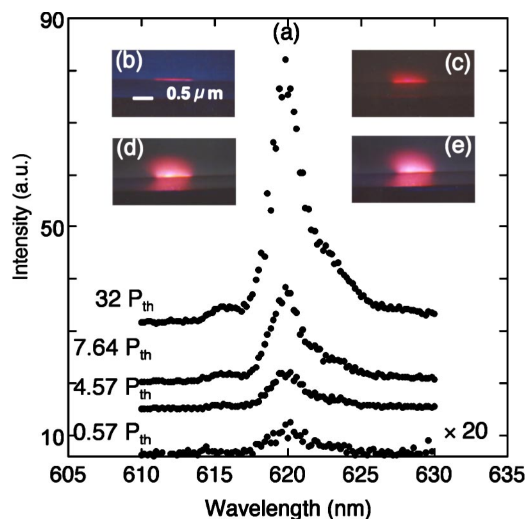

FIG. 2. (Color online), (a) Edge emission spectra from GaN:Eu 10-mm cavity for several pumping peak power densities (P_{th}=10 kW/cm^2). Photographs of edge emission from GaN:Eu cavities of various lengths at P_{in} =1.14 MW/cm^2: (b) 0.1, (c) 0.5, (d) 0.8, and (e) 0.9 cm.

Edge emission spectra from the 1-cm cavity length are shown in Fig. 2(a) at different pump peak powers. A sharp increase in output emission is observed as the pump power is increased beyond a certain level. No corresponding shift of the Eu^{3+} emission-peak wavelength is observed. In Figs. 2(b)–2(e), we observe that the red emission from the sample edge has a different intensity distribution at different excitation lengths. For the 1-mm cavity length, light emission is confined to the GaN:Eu thin-film active layer [Fig. 2(b)]. However, surface emission emerges for the longer cavity examples [Figs. 2(c)–2(e)].

We used the variable stripe length method[18] to measure the optical-modal gain of GaN:Eu. A one-dimensional amplification model (which excludes gain saturation effects) is used to obtain the modal gain values,

$$I = \frac{I_0 \times (l)}{g_{\mathrm{mod}}}(e^{g_{\mathrm{mod}} l} - 1), \quad (2)$$

where I is the measured amplified spontaneous emission, I_0 is the spontaneous emission intensity per unit area, l is the excitation length, and g_{mod}(cm^{-1}) is the net modal gain.

The inset diagram in Fig. 3 depicts the experimental configuration, including a traveling knife edge that defines the excitation region. The intensity increases exponentially with excitation length until the saturation length (l_s) is reached. To determine l_s, the derivative of the measured intensity (dI/dl) is plotted against the cavity length. This method shows that dI/dl increases until gain saturation, followed by a rapid decrease. Fitting Eq. (2) over the unsaturated gain region *only*, we obtain the small signal gain, which is effectively the net modal gain. Since material gain increases with pumping power, the sample excited with a higher pump power density has a shorter saturation length. Therefore, l_s is inversely proportional to the input power density. In our measurements, l_s varied from ~0.05 to ~0.1 cm depending on power density. At excitation lengths beyond l_s surface emission begins to occur [Figs. 2(c)–2(e)]. The solid line in Fig. 3 is a fit according to Eq. (2), yielding a net modal gain of 42.8 cm^{-1}. This modal gain value is higher than that typically measured[17] for dye lasers (1–10 cm^{-1}) and approximately

Downloaded 16 Nov 2004 to 129.137.207.245. Redistribution subject to AIP license or copyright, see http://apl.aip.org/apl/copyright.jsp

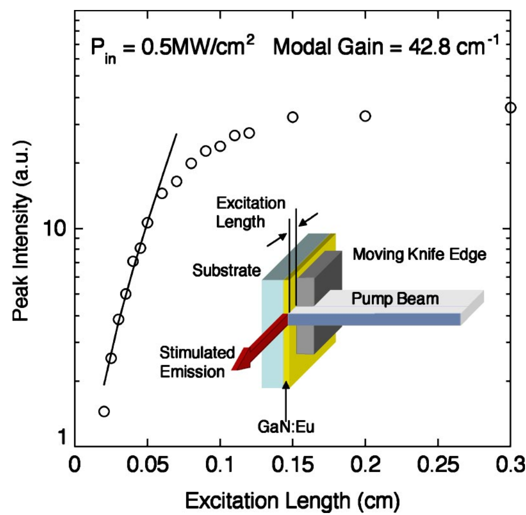

FIG. 3. (Color online), Peak emission (620 nm) vs excitation stripe length. The open circles are measured data and the solid line is fitted curve with one-dimensional amplifier model. Inset: schematic diagram of variable stripe length measurement.

the same as that reported[19] for 77-K operation of GaAs co-doped with Er and oxygen (45 cm^{-1}). Our value is also significantly higher than that reported[20] for Nd-doped glass (~0.07–0.15 cm^{-1}).

The optical modal loss at the peak wavelength is measured using the shifting excitation spot method.[21] The loss α in a semiconductor laser includes both external and internal contributions. The external loss is related to the resonator loss, such as reflection (largest term) and diffraction loss. The internal loss is mostly due to absorption by free carriers in the active and cladding layers and to scattering at interfaces.

The experimental configuration shown in Fig. 4 is similar to the gain measurement set up. A slit of 100-μm width replaces the knife edge to produce a region from which one can measure localized light emission. By moving the slit we can obtain optical loss values at the lasing wavelength. The relation between output intensity and distance is given by

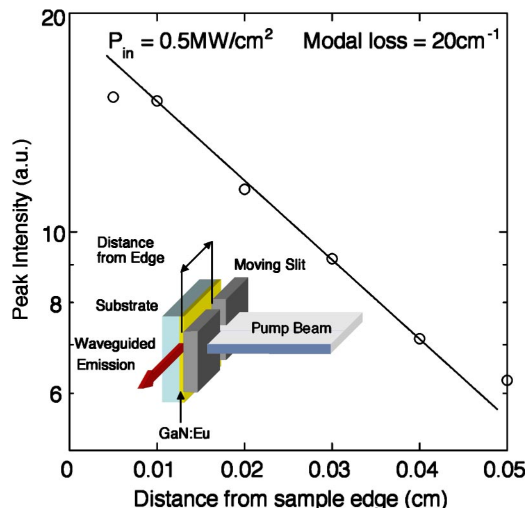

FIG. 4. (Color online), Optical loss at emission wavelength (620 nm) obtained by the SES method. The solid line is a fit to experimental data (open circles). Inset: schematic diagram of loss measurement.

$$I = I_0 e^{-\alpha l}, \tag{3}$$

where I_0 is the intensity generated by local excitation, α (cm^{-1}) is the internal loss coefficient (net modal loss), and l (cm) is the distance between the sample edge and the slit. The solid line in Fig. 4 is a fit according to Eq. (3), resulting in a calculated value of 20 cm^{-1} for the modal loss. This value is substantially higher than that reported[4] for undoped GaN (~1.23 cm^{-1}) at a similar visible wavelength (633 nm). The higher loss coefficient is probably due to scattering from crystal defects introduced by the heavy Eu concentration. Significantly lower loss can probably be achieved with improved growth conditions.

A simplified approach (based on bulk laser operation) allows us to calculate the approximate concentration of active optical centers using the material gain (modal gain + modal loss) and the SE cross section,

$$N^* = \frac{g_m}{\sigma_{ex}}. \tag{4}$$

For our GaN:Eu structure, we calculate $N^*(\mathrm{Eu}) \approx 9 \times 10^{20}/\mathrm{cm}^3$ or ~1 at. %. This value is of the same order of magnitude as the total Eu concentration in the GaN film.

RE-based lasing action in a semiconductor is demonstrated using optical pumping of a GaN:Eu thin-film cavity. The low SE threshold (~10 kW/cm^2) and the strong modal gain (~43 cm^{-1}) are positive indicators for obtaining electrically pumped lasing in this material system.

This work was supported in part by a contract with the U.S. Army Research Office (#DAAD19-03-1-0101). The authors are pleased to acknowledge the support, encouragement, and many technical discussions with J. M. Zavada.

[1] Mater. Res. Bull. Vol. 24 (1999).
[2] S. Nakamura and G. Fasol, *The Blue Laser Diode* (Springer, Berlin, 1997); H. Morkoc, *Nitride Semiconductors and Devices* (Springer, Berlin, 1999).
[3] A. J. Steckl, J. C. Heikenfeld, D. S. Lee, M. J. Garter, C. C. Baker, Y. Wang, and R. Jones, IEEE J. Sel. Top. Quantum Electron. **8**, 749 (2002).
[4] J. Heikenfeld, M. Garter, D.S. Lee, R. Birkhahn, and A. J. Steckl, Appl. Phys. Lett. **75**, 1189 (1999).
[5] H. Amano, T. Asahi, and I. Akasaki, Jpn. J. Appl. Phys., Part 1 **29**, 205 (1990).
[6] E. Nyein, U. Hömmerich, J. Heikenfeld, D. S. Lee, A. J. Steckl, and J. M. Zavada, Appl. Phys. Lett. **82**, 1655 (2003).
[7] U. Hömmerich, E. Nyein, D. S. Lee, J. Heikenfeld, A. J. Steckl, and J. M. Zavada, Mater. Sci. Eng., B **105**, 91 (2003).
[8] C-W. Lee, H. O. Everitt, D. S. Lee, A. J. Steckl, and J. M. Zavada, J. Appl. Phys. **95**, 7717 (2004).
[9] A. Yariv, *Quantum Electronics* (Wiley, New York, 1989), pp. 173–175.
[10] X. Zhao, S. Komuro, H. Isshiki, Y. Aoyagi, and T. Sugano, Appl. Phys. Lett. **74**, 120 (1999).
[11] G. R. Williams, S. B. Bayam, S. C. Rand, T. Hinklin, and R. M. Laine, Phys. Rev. A **65**, 013807 (2001).
[12] G. Fuxi, *Optical and Spectroscopic Properties of Glass* (Springer, New York, 1992), pp. 204–227.
[13] T. Y. Fan and R. L. Byer, IEEE J. Quantum Electron. **24**, 895 (1988).
[14] B. F. Aull and H. P. Jenssen, IEEE J. Quantum Electron. **18**, 925 (1982).
[15] S. A. Payne, L. L. Chase, L. K. Smith, W. L. Kway, and W. F. Krupke, IEEE J. Quantum Electron. **28**, 2619 (1992).
[16] R. Francini, F. Giovenale, U. M. Grassano, P. Laporta, and S. Taccheo, Opt. Mater. (Amsterdam, Neth.) **13**, 417 (2000).
[17] A. Kaminskii, *Laser Crystals* (Springer-Verlag, New York, 1981) p. 154.
[18] K. L. Shaklee, R. E. Nahory, and R. F. Leheny, J. Lumin. **7**, 284 (1973).
[19] P. Eliseev, S. Gastev, A. Koizumi, Y. Fujiwara, and Y. Takeda, Proc. SPIE **4645**, 35 (2002).
[20] F. Gan, *Laser Materials* (World Scientific, Singapore, 1975), p. 324.
[21] J. Valenta, I. Pelant, and J. Limmros, Appl. Phys. Lett. **81**, 1396 (2002).

Downloaded 16 Nov 2004 to 129.137.207.245. Redistribution subject to AIP license or copyright, see http://apl.aip.org/apl/copyright.jsp